PAPER Nr. : 11

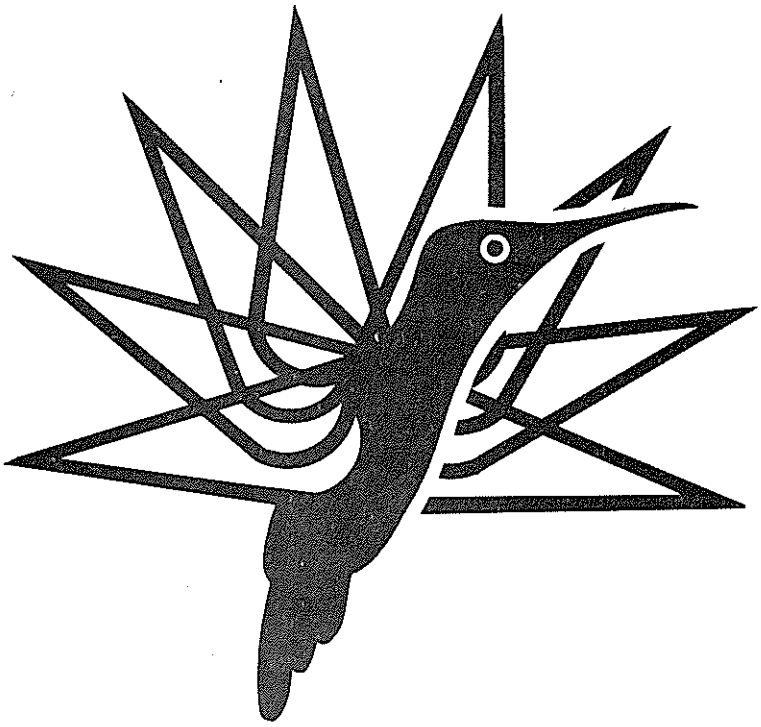

THE AERODYNAMIC CHARACTERISTICS OF SOME NEW RAE BLADE SECTIONS, AND THEIR POTENTIAL INFLUENCE ON ROTOR PERFORMANCE

by

P. G. Wilby
Royal Aircraft Establishment
Farnborough, England

FIFTH EUROPEAN ROTORCRAFT AND POWERED LIFT AIRCRAFT FORUM
SEPTEMBER 4 – 7TH 1979 - AMSTERDAM, THE NETHERLANDS

THE AERODYNAMIC CHARACTERISTICS OF SOME NEW RAE BLADE SECTIONS, AND THEIR POTENTIAL INFLUENCE ON ROTOR PERFORMANCE

by

P G WILBY

ROYAL AIRCRAFT ESTABLISHMENT, FARNBOROUGH, UK

ABSTRACT

The values of $C_{L_{MAX}}$ and C_{m_o}, and the drag characteristics, are given for several new RAE profiles and NACA 0012, as measured in steady conditions. Results from oscillatory tests are then presented for RAE 9647 (one of the new sections) and NACA 0012. These show that at M = 0.3 the gain in $C_{L_{MAX}}$ for the new section relative to NACA 0012 is considerably greater in dynamic conditions than in steady conditions. Dynamic tests are seen to be necessary for the full assessment of new profiles. The effect of section characteristics on rotor performance is evaluated by means of a rotor performance calculation that incorporates a model of dynamic stall; the predicted onset of blade stall providing a criterion for determing the rotor thrust limits. The new sections are seen to offer a 35% increase in rotor thrust capability, relative to rotors with the NACA 0012 section.

1 Introduction

In recent years a series of aerofoils has been designed at the RAE especially for use as helicopter rotor blade sections. This paper summarizes the aerodynamic characteristics of some of these new profiles and outlines the philosophy behind their designs. The information required for a proper assessment of the sections is discussed together with the predicted effect of such sections on rotor performance.

The overall aim of the research into blade section design was to derive new profiles that will delay the onset of retreating blade stall and thereby permit a rotor of given size to generate more lift (in forward flight), without detriment to control loads. Such a blade section would allow smaller rotors to be used to achieve a given speed and thrust combination, giving benefits in reduced rotor mass (and hence increased payload for a given total mass) and reduced profile power.

2 Aerofoil Characteristics in Steady Flow

In this section, the aerodynamic characteristics of some of the RAE aerofoils will be presented, as measured in steady conditions.

The measurements were obtained in the aerofoil tunnel at the Aircraft Research Association (ARA) in the UK. This tunnel has a test section which is 45 cm high and 20 cm wide with slotted upper and lower walls of open area ratio 0.03. The model aerofoils spanned the width of the tunnel and had a chord of 12.5 cm. Surface pressure was measured at 45 positions around the model, with lift and pitching-moment obtained from integration of pressures. Drag was obtained from wake measurements using a pitot rake. The tunnel was pressurized to give a Reynolds number of $M \times 10^7$, which is close to full scale value, for Mach numbers up to 0.65. Above $M = 0.65$, the Reynolds number was held constant at 6.5×10^6. Tests were carried out with transition fixed by a band of Ballotini balls at 7% chord, and also with free transition. The range of test Mach numbers was 0.3 to 0.875.

One of the usual aims in aerofoil design is to achieve a high value of $C_{l_{MAX}}$, so as to delay the onset of retreating blade stall in both level flight and low speed manoeuvres. Figure 1 therefore gives the values of $C_{l_{MAX}}$ for a representative selection of the aerofoils, at $M = 0.4$ and 0.5. Results for the NACA 0012 aerofoil are included to serve as a datum, but results published by other authors for other aerofoils are not included because of the difficulties of trying to compare measurements from different wind-tunnels. It is well known that widely different values of $C_{l_{MAX}}$ can be obtained for a given aerofoil in different tunnels.

To achieve a high value of $C_{l_{MAX}}$ one needs to incorporate camber into the aerofoil design, in the form of nose-droop, but this tends to produce a nose-down pitching-moment at zero lift. The latter must be minimized because of its adverse effects on control

loads, and has been controlled in the RAE aerofoils through reflex camber over the rear of the profiles. One of the aims of the research programme was to test various combinations of nose droop and reflex camber, and study the trade-off between $C_{L_{MAX}}$ and C_{m_o}. Figure 1 also gives the measured values of pitching-moment coefficient at zero-lift for the aerofoils over the upper range of test Mach numbers. The increase in magnitude of the pitching-moment, as Mach number increases, is a further effect of amber and accentuates the influence of camber on control loads. Thus, although the RAE 9647 aerofoil has effectively zero pitching-moment at low values of Mach number it can still be expected to produce some increase in control loads, relative to a symmetrical blade section, on a rotor at high forward speeds. However, it produces gains in $C_{L_{MAX}}$ of 30% and 36% at M = 0.4 and 0.5 respectively, relative to the NACA 0012 profile. The less cambered RAE 9644 aerofoil has a reduced value of pitching-moment but also a smaller gain in $C_{L_{MAX}}$. The RAE 9645 aerofoil has the same degree of nose-droop as the RAE 9647 section but differences in the forward upper surface shapes and in rear loading give it an appreciably higher value of $C_{L_{MAX}}$ at M = 0.4 (an increase of 40% over NACA 0012). However, this is at the expense of a larger value of nose-down pitching-moment. With the thinner RAE 9634 aerofoil the magnitude of C_{m_o} is relatively low as a result of the restricted extent of nose-droop that can be introduced on a thinner aerofoil without incurring excessive drag creep at low values of C_L. This means that the gains in $C_{L_{MAX}}$ are much smaller than for the RAE 9647 section.

Figure 2 shows the variation of drag coefficient with Mach number at zero lift for the various sections, and it is seen that only the RAE 9634 aerofoil gives a delay in drag-rise relative to the NACA 0012 profile. With the thicker sections, the introduction of camber has led to a drag penalty at the higher values of Mach number that can be encountered at the tip of the advancing blade. It is also important to maintain as low a value of drag as possible near the blade tip in hover, and over the outer part of the blades in the fore and aft sectors of the rotor disc in forward flight. With this in mind, the variation of drag coefficient with lift coefficient is shown in Figure 3 at Mach numbers of 0.55 and 0.6. All the RAE sections are seen to delay drag rise to a higher value of lift coefficient - an essential feature for blade sections which are intended to increase the blade loading of a rotor.

The study of steady flow aerofoil characteristics is of considerable interest and value, but on its own it can not tell us whether or not a particular aerofoil has the optimum combination of characteristics that would make it the best choice for a rotor blade section. A true assessment can only be made on the basis of knowledge of the conditions that are encountered on a rotor in whatever mode of flight is considered to be most important. For the purposes of this

paper we will assume that level cruising flight (with adequate margin for manoeuvre) is the critical condition, and that it is desired that the cruise speed should be at least 140 knots. With a conventional tip speed of about 200 m/sec, we quickly see that the value of $C_{L_{MAX}}$ at $M = 0.3$ is of much more importance than that at $M = 0.4$ or 0.5, as far as retreating blade stall is concerned. One problem we then encounter is that it is particularly difficult to obtain the true value of $C_{L_{MAX}}$ for aerofoils such as the commonly used NACA 0012 when Mach number falls below 0.4, as the measured value becomes very sensitive to test conditions. This can be seen in the results presented in Figure 4 for the measured variation of lift coefficient with incidence, as measured in the ARA wind-tunnel. Considerable differences in $C_{L_{MAX}}$ were found even in two tests where the test conditions were set up to be identical. This of course makes it impossible to obtain a reliable assessment of the gain in $C_{L_{MAX}}$, at this important value of Mach number, that is provided by new aerofoils. On further reflection however, we realize that on the helicopter rotor retreating blade stall is dynamic in nature, and steady flow values of $C_{L_{MAX}}$ are not necessarily the important quantity. The feature of retreating blade stall that sets a limit to rotor thrust is the large and sudden change in pitching-moment, that leads to large fluctuations in blade torsional loads and in pitch-control loads. In order to attain high values of rotor thrust we need a blade section that can reach high values of incidence, in oscillatory conditions, without involving the large changes in pitching-moment associated with dynamic stall. The value of C_L that is attained when this pitching-moment break occurs on the retreating blade is of no special importance in its own right; the important factor being the magnitude of the lift being produced by the other blades over the fore and aft sectors of the disc (where the major contributions to rotor thrust are to be found). Clearly, in order to assess the merits of an aerofoil we need to test it in oscillatory conditions. Then we need to be able to run a rotor experiment or a calculation to find out what value of rotor thrust is being generated when the pitching-moment break is encountered by the retreating blade. Such a calculation would of course need to incorporate a faithful representation of the dynamic stall characteristics of the blade section.

3 Dynamic Stall Characteristics

An oscillatory aerofoil test rig has been designed and built at ARA for the purpose of testing the new RAE blade sections and studying their dynamic stall characteristics. Some results from tests on the RAE 9647 and NACA 0012 aerofoils are presented here to illustrate the importance of oscillatory characteristics. In these tests, the model spans the width of the tunnel, has a chord of 10 cm and is fitted with pressure transducers measuring absolute pressure at 32 stations around the profile. Normal force and pitching-moment are obtained by integration of the measured pressures.

Figures 5 shows the measured variation of normal force coefficient C_N and pitching-moment coefficient C_m with incidence for a selection of sinusoidal pitching-cycles at a Mach number of 0.3. For the cases shown, the amplitude of the pitch oscillations was 8.5° and the reduced frequency was that corresponding to typical once per revolution on a full scale rotor. Mean incidence is progressively increased to take both aerofoils through the point of stall onset. The fact that the RAE 9647 aerofoil can reach higher incidences than the NACA 0012, without encountering stall, is clearly seen. Figure 6 shows an analysis of several cases at the some frequency and amplitude as those in Figure 5, but also includes cases at Mach numbers close to 0.4. Here, the maximum deviation in C_m from its pre-stall single loop is plotted against the maximum value of incidence attained in the cycle. The measured values of C_m deviation (or ΔC_m) are shown as small circles and of course lie on the line $\Delta C_m = 0$ for conditions that do not encounter stall. As the stall incidence is exceeded, the value of ΔC_m becomes progressively larger. On drawing a line through the measured points, a clearly defined break point is obtained, and the value of incidence at this break point (to be referred to as the critical value) is 2.5° greater for the RAE 9647 aerofoil than for the NACA 0012 profile. Before proceeding, we must be quite clear as to the significance of this break point. The results show that once the critical value of incidence has been exceeded, then there will unavoidably be a break in the value of pitching moment. The break in pitching-moment will not necessarily occur at the critical value of α, and we can in fact expect a significant delay in the pitching-moment break if $\dot{\alpha}$ is large when the critical value of α is reached. A brief examination of such delays, due to dynamic effects, is now useful in gaining a further appreciation of the significance of the critical value of incidence.

In Beddoes analysis[1] he concluded that in dynamic conditions there will be a break in pitching-moment at the end of a certain interval of time after passing the value of incidence α_1 at which a pitching-moment break occurs in steady conditions, provided that the value of incidence is still in excess of α_1. Beddoes gave the value of this time delay as

$$\Delta t = \frac{2.44c}{V}$$

where c is the aerofoil chord and V the free stream velocity. Now the ARA dynamic rig is capable of producing ramp like variations of incidence (following the suggestions of Beddoes) as well as oscillatory motions, and these ramp motions, at different values of $\dot{\alpha}$ are of great value in studying time delays. Figure 7 shows some measured variations of pitching-moment coefficient with incidence for a series of ramp rates, at two values of Mach number, and clearly the value of α at which the pitching-moment break occurs increases with $\dot{\alpha}$. As a clear measure of pitching-moment break let us take the values of α for which the value of C_m has fallen by 0.05 below the maximum

value reached, and plot them against $\frac{c}{V}\alpha$, as in Figure 8, then the slope of the resulting line will be equal to n_1

$$\text{where } \Delta t = \frac{nc}{V} \quad .$$

The value for n obtained from Figure 8 is 2.7 which agrees quite well with the value given by Beddoes[1]. With this concept confirmed, let us now return to the critical values of α obtained in Figure 6 from the oscillatory tests with 8.5° amplitude and 25 Hz frequency. For the NACA 0012 aerofoil, at M = 0.3, the critical value of incidence was found to be 15°, and in Figure 9 we plot the variation of α with time for the case where this critical value is only just reached. As this is the maximum value of incidence that can be attained without inducing a break in pitching-moment, then the elapsed time between passing above the value of incidence for steady flow pitching-moment break, α_1, and passing back below α_1 must be $\frac{2.7c}{V}$. This time interval is marked on Figure 9, showing that there is no significant difference between α_1 and the critical value of α given by the plots in Figure 6.

Having reached the above conclusion it is interesting to plot in Figure 10 the variation of C_m with α, as measured in steady conditions, for both the NACA 0012 and RAE 9647 aerofoils at M = 0.3 and 0.4. Marked on these plots is the value of α_1 deduced from oscillatory tests. This is seen to be substantially greater than the value indicated by the steady test results for the RAE 9647 aerofoil, but only slightly greater in the case of the NACA 0012 section. The conclusion to be reached here is that the benefits of the RAE 9647 aerofoil in delaying the onset of dynamic stall, beyond that experienced with the NACA 0012 profile, would be greatly underestimated on the basis of steady test results. Dynamic tests are necessary if a true assessment of an aerofoil's characteristics is to be obtained.

It should now be noted that Beddoes[3] has recently found that the steady flow pitching-moment break criterion leads to a prediction of premature dynamic stall for some aerofoils at low value of Mach number ($M < 0.35$). For these lower values of Mach number he now recommends a criterion based on predicted leading-edge pressure distributions. The resulting calculated value of the critical incidence is then in some cases higher than the value of α_1 taken from steady flow measurements. The results of the oscillatory tests on the RAE 9647 aerofoil thus support the conclusion that the steady flow pitching-moment break criterion is inadequate at low values of Mach number, but also suggest that this is still the case at M = 0.4. However, at this value of Mach number, the upper surface flow near the leading-edge is supercritical (at high angles of incidence) with a discontinuous pressure rise at a shock standing typically at about 5% chord. It is thus not possible to extend the leading-edge pressure criterion, which involves the pressure gradient aft of the suction peak, to this value of Mach number.

Similar results have been obtained from oscillatory tests on the RAE 9644 aerofoil, and several other members of the new aerofoil family will now be tested in dynamic conditions. As a further check on dynamic stall behaviour, a part of one blade of the RAE Puma research helicopter has been modified to permit a fairing of RAE 9647 profile to be added. An array of pressure transducers will provide measurements of chordwise pressure distributions from which normal force and pitching-moment can be derived. By setting this fairing at an incidence of 2^{o} relative to the standard blade it is expected to be able to force the RAE 9647 fairing into stalled conditions, and then compare the variation of C_m against C_N with that measured in the two-deminsional wind-tunnel tests.

4 Effect of Section Characteristics on Predicted Forward Flight Performance

One of the main aims in the analysis of dynamic stall by Beddoes was to provide a theoretical model that could be incorporated in the rotor loads and performance programs that have been largely developed at Westland Helicopters. These programs are used at the RAE and results given by the rotor loads program are compared with flight measurements on a Puma helicopter by Brotherhood and Young[2] in another paper at this Forum. In that paper it is shown that the onset of retreating blade stall is quite accurately predicted by theory when the dynamic stall model is included. Here, a program that includes the dynamic stall model, but assumes rigid blade flapping with the 1st torsional mode, will be used to assess the effect of blade section design on rotor performance. In these calculations the wake is represented by a series of vortex rings as described in Ref 2, and the values of α_1 used in the modelling of dynamic stall are those derived from oscillatory aerofoil tests.

For these performance calculations we will take a rotor of the dimensions and characteristics of a Westland Sea King rotor, with a tip speed of 207 m/sec and, in the first instance, a forward speed of 140 knots. It is found that for blades of NACA 0012 profile, dynamic stall onset is predicted to occur when the rotor thrust coefficient reaches the value of 0.086 σ, and the predicted variation of C_m with α at 0.85 R, for the retreating blade, is given in Figure 11. We see that the maximum predicted value of incidence of 15^{o} is attained at $\psi = 270^{o}$, where the local blade Mach number is 0.3. The predicted break in the value of C_m at this point reproduces that observed in the oscillatory aerofoil experiments (see Figure 6). Figure 11 also shows the predicted variation of C_m with α when the rotor thrust coefficient has been increased to 0.10 σ, and, in line with oscillatory aerofoil test results, the magnitude of the fall in value of C_m has greatly increased due to the increased severity of the dynamic stall. The dramatic change in predicted blade root torsional load on increasing rotor thrust coefficient from 0.086 σ to 0-10 σ is shown in Figure 12, and is a direct result of retreating blade stall. This consequence of blade stall has been clearly measured in flight on a Puma helicopter at the RAE, as reported in Ref 2.

On the basis of the aerofoil test results discussed earlier it can be expected that a change in blade section, to the RAE 9647 profile for instance, will provide a considerable increase in the value of thrust at stall onset. With this blade section, the rotor performance program predicts that the retreating blade will be on the verge of stall at $\frac{C_T}{\sigma} = 0.116$, which represents a 35% increase over the corresponding value for the rotor with NACA 0012 blade section. Figure 13 shows the predicted variation of incidence over the outer part of the retreating blade. At 0.85 R, the maximum value of α is attained at $\psi = 273^\circ$ where the blade Mach number is very close to 0.3, and this value of α is exactly 17.5° which is the maximum value that was reached in the oscillatory aerofoil tests without provoking stall. For larger values of thrust coefficient, a rapid increase in oscillatory root torsional load can be expected. However, at $\frac{C_T}{\sigma} = 0.116$, the predicted peak to peak variation of root torsional load, as shown in Figure 14, is only 30% higher than it is for the NACA 0012 blades at $\frac{C_T}{\sigma} = 0.086$, inspite of the fact that the RAE 9647 aerofoil is cambered. This section was of course designed to have a value of C_{m_o} that is close to zero at low values of Mach number. However, the magnitude of C_{m_o} does become rapidly larger as Mach number approaches 0.8. For the rotor case under consideration, the value of Mach number at $\psi = 90^\circ$ and $y/R = 0.95$ is 0.79, where $C_{m_o} = -0.025$ in steady conditions, and this provides an explanation for the increase in nose-down torsional load that is predicted for the advancing blade (Figure 14). Obviously, as rotor forward speed increases beyond 140 knots one can expect to find a further increase in peak-to-peak blade torsional load for a rotor with RAE 9647 blade section. Attention must also be paid to conditions over the fore and aft sectors of the rotor disc, when ideally the blade should not be operating far into drag-rise. Figure 15 gives some guidance on this matter as it shows the variation of C_D with α as measured for the RAE 9647 aerofoil in steady test conditions at Mach numbers of 0.5 and 0.55. These are the values of blade Mach number at 0.8 R and 0.9 R, for the particular rotor case in question, at azimuth angles of 0° and 180°. Marked on these curves are the values of incidence predicted by the rotor performance program for $\frac{C_T}{\sigma} = 0.086$. These values of incidence are seen to be below the values at which the steep drag-rise begins, except for the case of 0.9 R at $\psi = 0^\circ$. However, one can not expect the steady values of C_D to hold on the rotor at 0° and 180° azimuth where the value of $\dot{\alpha}$ is high and there will be a considerable distortion of the pressure distributions. At the values of Mach number of interest the drag-rise is essentially a consequence of the development of supercritical flow, with drag being dependent upon the strength and position of the shock wave. As pitch rate will considerably affect the strength and position of the shock, as seen in the results for an oscillatory pitch experiment in Figures 16 and 17, we can expect an appreciable effect on drag. It is however very difficult to measure drag in dynamic conditions, and has not been possible with the ARA rig.

There is therefore an absence of data on this important effect, but nevertheless an attempt has been made to represent this effect in the WHL rotor performance program.

Let us now move on to a case with the higher forward speed of 170 knots. At $\frac{C_T}{\sigma} = 0.086$ (the same value as for the limiting case with NACA 0012 section at a speed of 140 knots) the azimuthal variation of blade root torsional load has been plotted in Figure 18, taking the blade section to be the RAE 9647 aerofoil. As expected, there has been an increase in the nose-down load over the advancing sector of the disc, but further calculations show that this can be reduced appreciably by a change of section over the outer part of the blade. The second curve in Figure 18 is for blades with the RAE 9647 section out to 0.85R with a linear change to the RAE 9634 section at 0.95R. As seen in Figure 1, the magnitude of C_{m_o} for the RAE 9634 aerofoil is much smaller than for the RAE 9647 profile at the higher values of Mach number. Being a thinner section, the change in profile near the blade tips brings a 3.5% reduction in power required. With this rotor configuration, Figure 19 suggests that there is not likely to be any particular drag problem over the fore and aft sectors of the disc. Also, Figure 20 shows that the retreating blade is operating well below stall onset, with the maximum value of incidence attained at 0.85R (where the section is RAE 9647) being just under 15°. The maximum incidence attainable without stall being about 17.5° at M = 0.3 (see Figure 6). However, at 0.95 R where the section is the RAE 9634 profile, the maximum incidence attained is 14° which is only 1° below the expected value for stall onset. The possibility that now comes to mind is that of introducing some non-linear twist over the outer part of the blade in order to lower the value of incidence outboard of 0.85R on the retreating blade. This would then allow an appreciably higher value of thrust to be generated without provoking stall. Alternatively, a still higher value of forward speed should be attainable at the same value of thrust coefficient.

Clearly one can only have confidence in the above results if one has confidence in the method used for predicting rotor performance, blade incidence and the effects of blade stall on root torsional loads. It is in order to gain this confidence that the flight test programme, described in Ref 2, was set up.

5 Tail Rotor Blade Sections

Special aerofoils for use as tail rotor blade sections have also been designed at the RAE, as the requirements and constraints are somewhat different than for main rotor blade sections. In the first place, emphasis can be placed on the attainment of the highest possible value of $C_{L_{MAX}}$ at Mach number appropriate to tip region of the blade in hover. This is to cater for the occasional demands for high thrust in hover or sideways flight manoeuvres when high yaw accelerations are called for. In the second place, it has long been recognised that larger values of C_{m_o} can be tolerated on tail rotor blades than can be accepted on main rotor blades.

Figure 21 shows values of $C_{L_{MAX}}$ and C_{m_o} for two tail rotor sections, as measured in steady wind-tunnel tests at ARA, at a value of Reynolds number appropriate to tail rotor blades. The RAE 9670 section is seen to give a 35% increase in $C_{L_{MAX}}$ over that for the NACA 0012 profile at $M = 0.55$ (approximately the value of Mach number at the radial position of the maximum blade incidence in hover), with the RAE 9671 section providing a gain of almost 50% at the cost of a small increase on the magnitude of C_{m_o}. The RAE 9670 aerofoil incorporated a trailing-edge tab over the last 7% of the chord, and tests were carried out to measure the effect of tab deflections on $C_{L_{MAX}}$ and C_{m_o}. Results for a 4^o tab deflection are included in Figure 21.

Successful flight tests have been carried out by Westland Helicopters on a Sea-King helicopter with a tail rotor of RAE 9670 section, as reported in Ref 4, with considerable gains in tail rotor thrust measured.

6 Conclusions

Some examples of aerofoil characteristics and their effect on predicted rotor performance have been given, to serve as illustrations of the many aspects that must be considered in assessing the merit of new blade sections. Oscillatory aerofoil tests and a reliable method for predicting both blade incidence and the effects of stall are essential in the prediction of the influence of section designs on rotor performance. Appropriate rotor experiments are necessary in order to decide on the reliability of the prediction method.

Using the experimental evidence and prediction methods that are available it is concluded that new blade sections can increase the maximum lift capability of a rotor in cruising flight by about 35%, or raise the limiting cruise speed by more than 20%, relative to a rotor with NACA 0012 blade sections.

References

1 T S Beddoes, A synthesis of unsteady aerodynamic effects including stall hysteresis, Proceedings of First European Rotorcraft and Powered Lift Forum, Southampton, 1975

2 P Brotherhood, C Young, The measurement and interpretation of rotor blade pressures and loads on a Puma helicopter in flight, Proceedings of Fifth European Rotorcraft and Powered Lift Forum, Amsterdam, 1979.

3 T S Beddoes, Onset of leading-edge separation effects under dynamic conditions at low Mach number, Paper presented at 34th Annual National AHS Forum, 1978.

4 C V Cook, The flight evaluation of a highly cambered tail rotor, Proceedings of Second European Rotorcraft and Powered Lift Forum, Buckeburg, 1976.

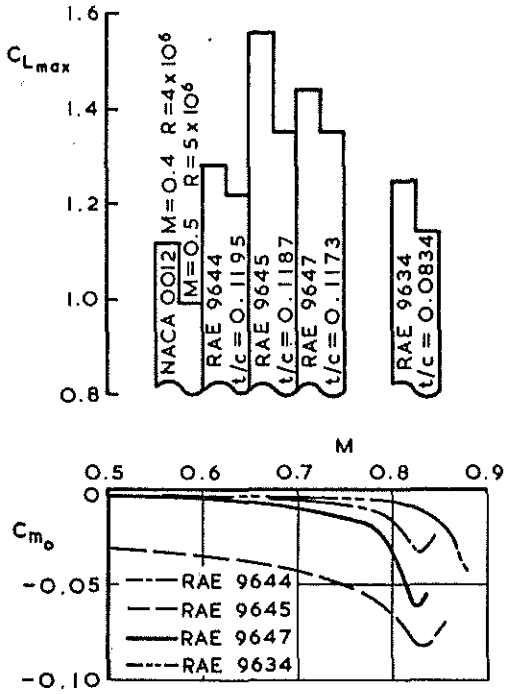

Fig 1 Measured values of maximum lift coefficient and pitching moment coefficient at zero lift

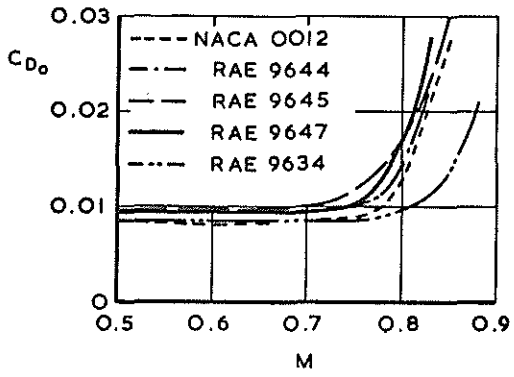

Fig 2 Measured variation of drag coefficient at zero lift with Mach number

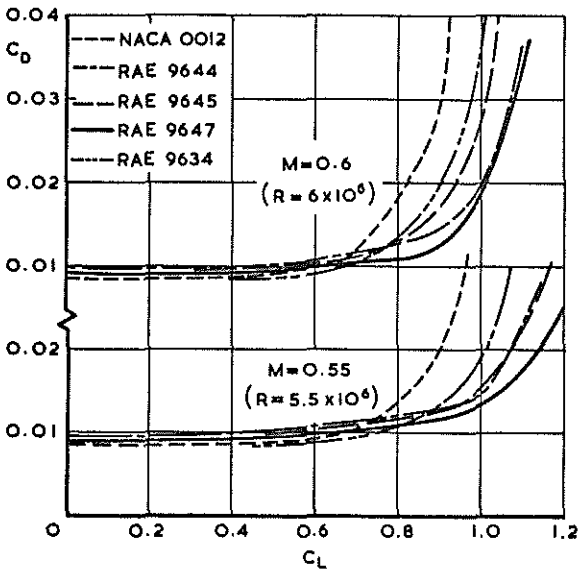

Fig 3 Measured variation of drag coefficient with lift coefficient

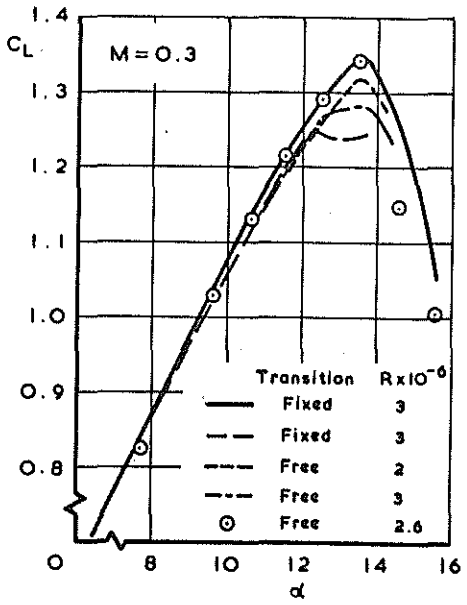

Fig 4 Variation of lift coefficient with incidence measured on NACA 0012

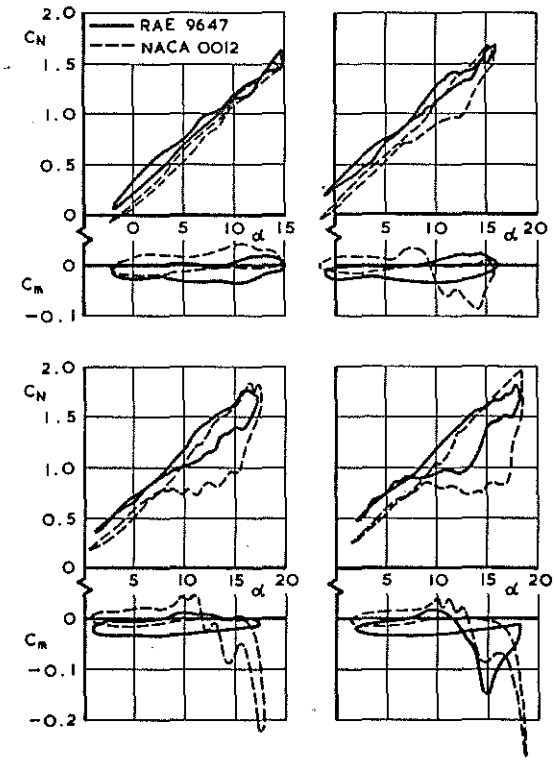

Fig 5 Measured variation of C_N and C_m during oscillatory pitching motion at M = 0.3 and 25 Hz

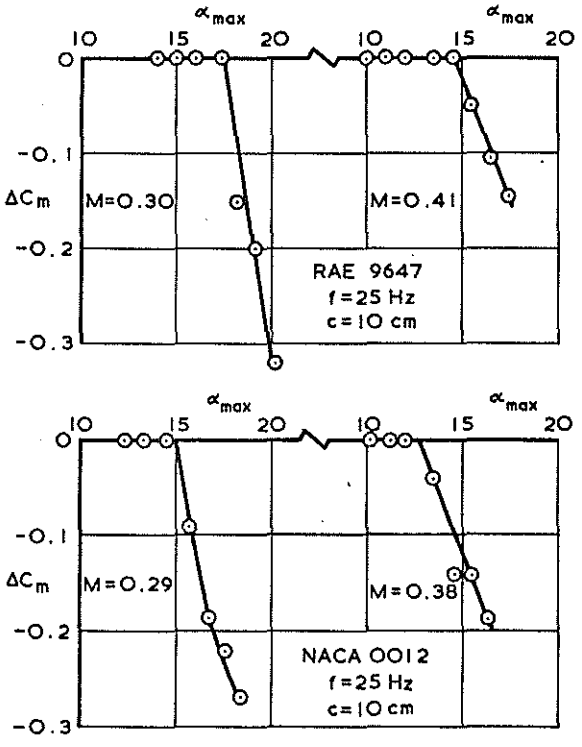

Fig 6 Maximum deviation in C_m, during an oscillatory pitch cycle, as a function of maximum incidence

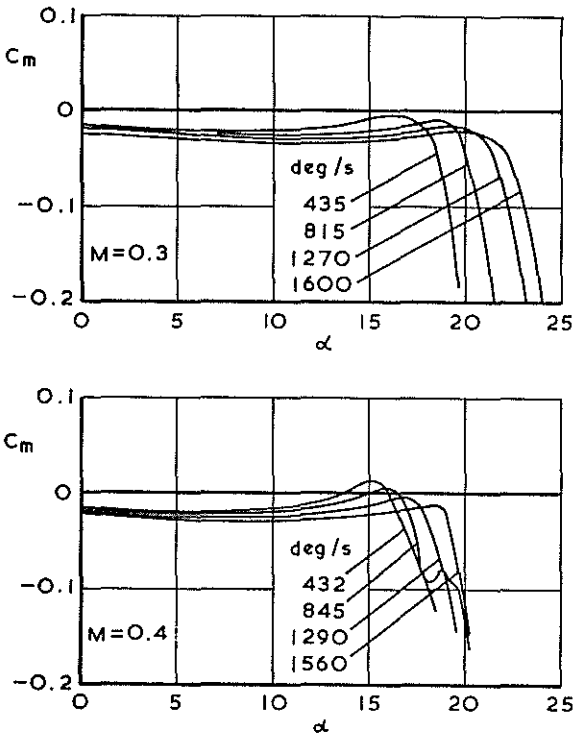

Fig 7 Variation of C_m with α measured on RAE 9647 aerofoil during ramp pitch motion

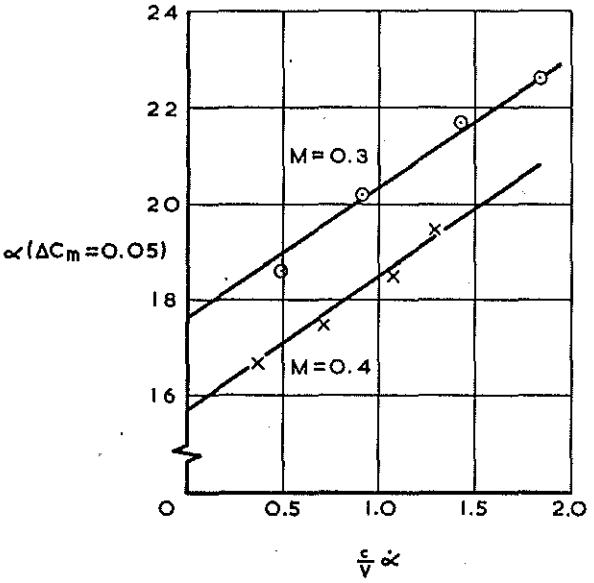

Fig 8 Incidence for which C_m has fallen by 0.05, plotted against non-dimensional pitch rate, for cases in Fig 7

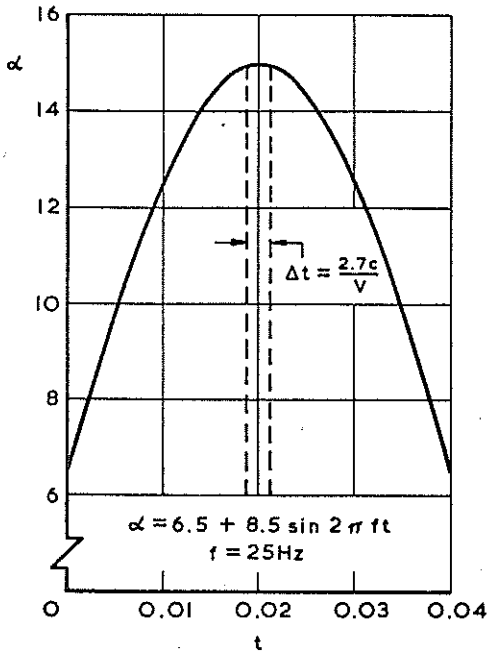

Fig 9 Variation of incidence with time in sinusoidal pitch variation during which the maximum incidence attained is the maximum incidence that can be reached without stall occurring

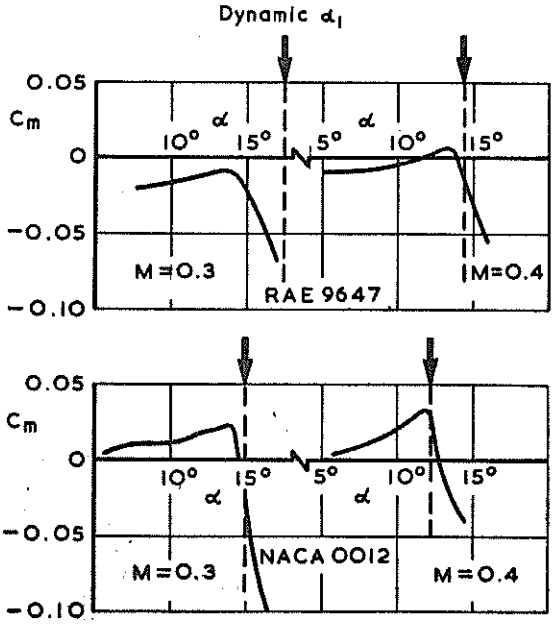

Fig 10 The variation of C_m with α as measured in steady conditions, with α_1 as deduced from dynamic tests indicated

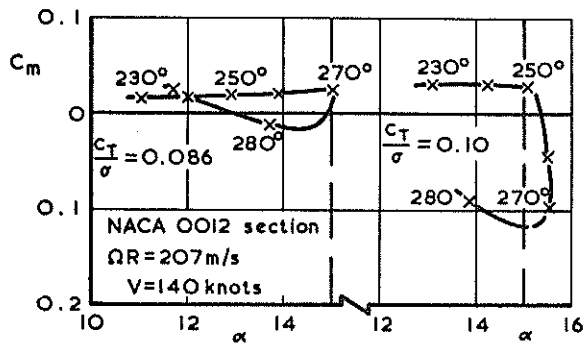

Fig 11 Variation of C_m with α at 0.85R on retreating blade as predicted by rotor performance program

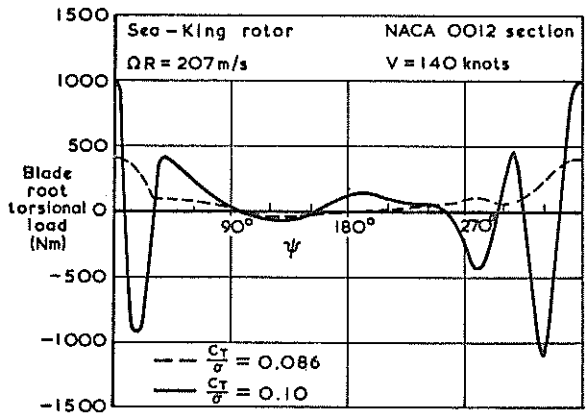

Fig 12 Predicted variation of blade root torsional load with azimuth

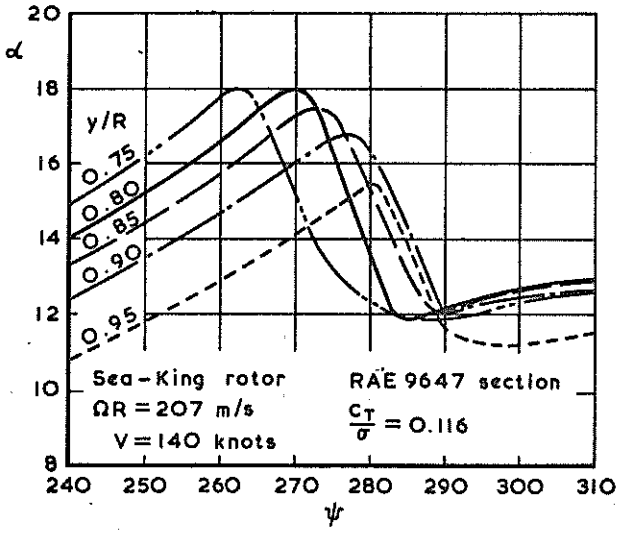

Fig 13 Variation of blade incidence with azimuth as predicted by rotor performance program

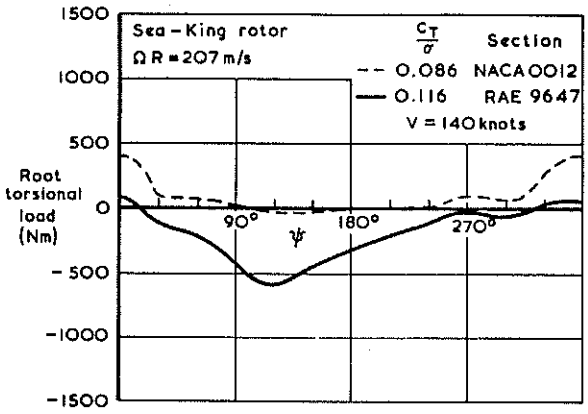

Fig 14 Predicted variation of blade root torsional load with azimuth

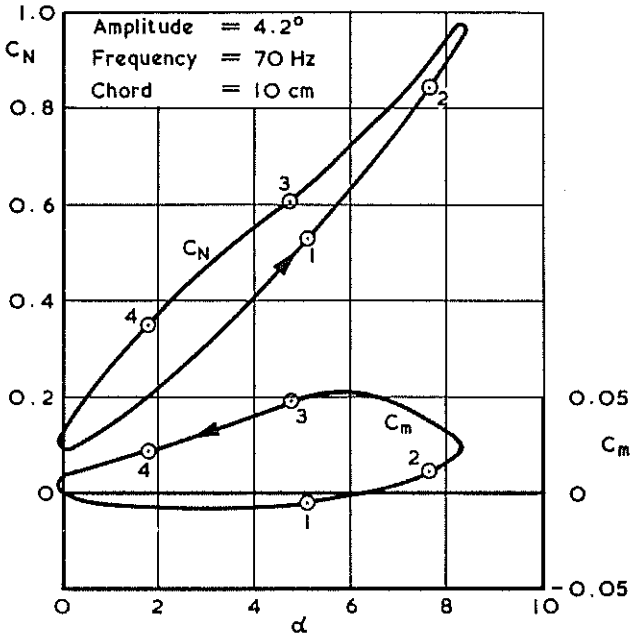

Fig 16 Variation of C_N and C_m as measured on NACA 0012 in oscillatory pitching motion at M = 0.61

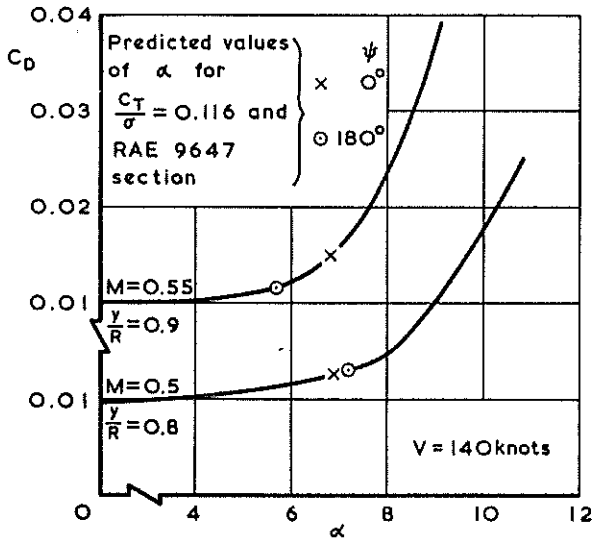

Fig 15 Variation of C_D with α as measured in steady conditions for the RAE 9647 aerofoil at Mach numbers encountered at y/R = 0.8 and 0.9 for $\psi = 0^o$ and 180^o

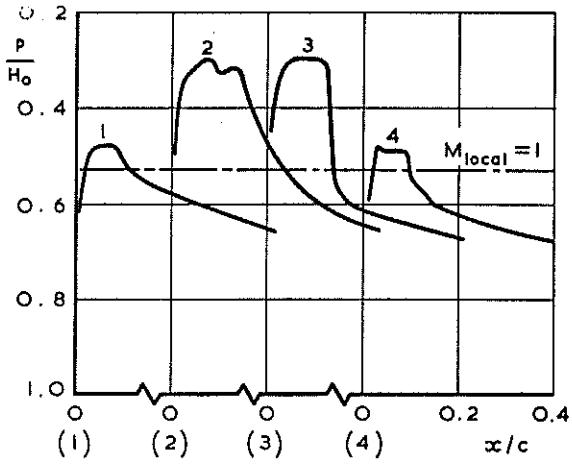

Fig 17 Measured pressure distributions over forward upper surface of NACA 0012 at four points in the pitch cycle shown in Fig 16

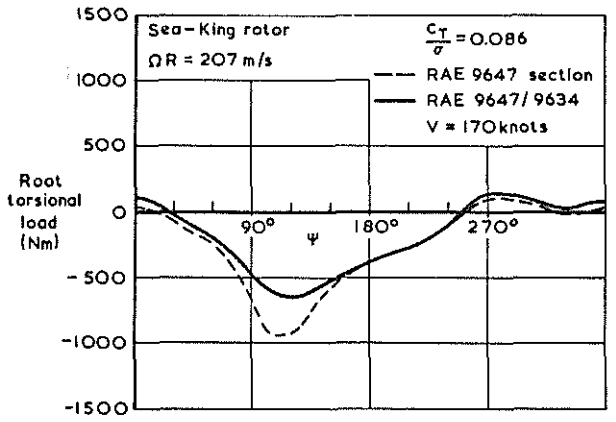

Fig 18 Predicted variation of blade root torsional load with azimuth

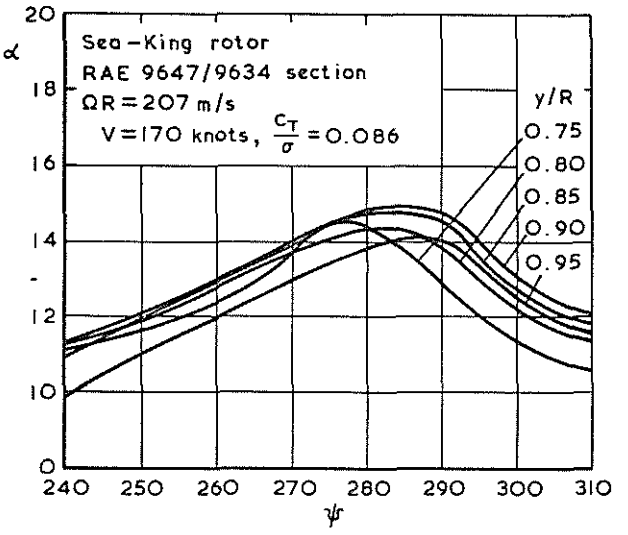

Fig 20 Predicted variation of blade incidence with azimuth and radial station

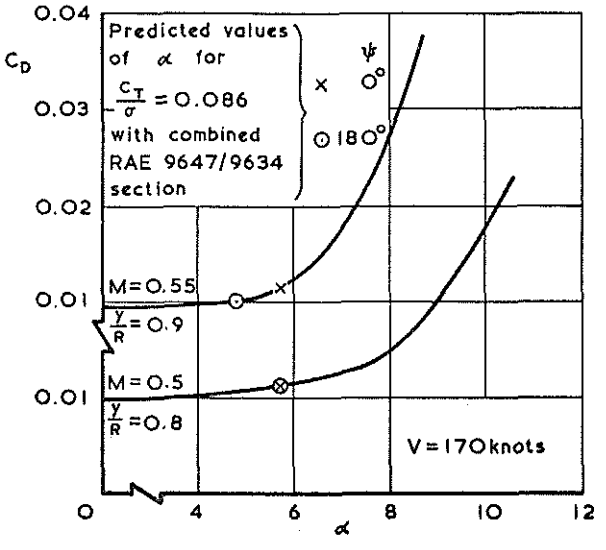

Fig 19 Variation of C_D with α for blade sections in steady conditions at Mach numbers encountered at 0.8R and 0.9R for $\psi = 0^0$ and 180^0

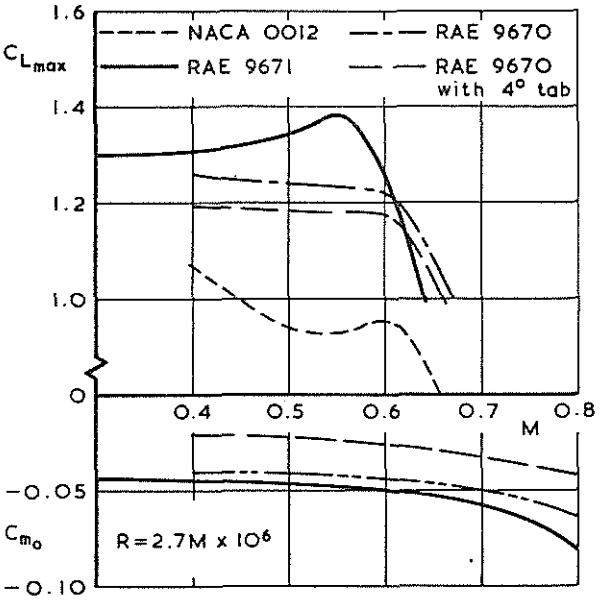

Fig 21 Variation of $C_{L_{max}}$ and C_{m_0} with Mach number as measured in steady conditions for tail rotor blade sections